Available online at www.sciencedirect.com
SCIENCE DIRECT®
Biochimie 85 (2003) 1007–1016
BIOCHIMIE
www.elsevier.com/locate/biochi

^{1}H NMR studies of the effect of mutation at Valine45 on heme microenvironment of cytochrome b_5

Chunyang Cao [a], Qi Zhang [a], Zhi-Qiang Wang [b], Yue-Feng Wang [a], Yun-Hua Wang [b], Houming Wu [a,*], Zhong-Xian Huang [b,*]

[a] *State Key Laboratory of Bio-organic and Natural Products Chemistry, Shanghai Institute of Organic Chemistry, Chinese Academy of Sciences, 354 Feng Lin Lu (Road), Shanghai 200032, China*
[b] *Chemical Biology Laboratory, Department of Chemistry, Fudan University, Shanghai 200433, China*

Received 12 April 2003; accepted 18 August 2003

Abstract

1D and 2D ^{1}H NMR were employed to probe the effects on the heme microenvironment of cytochrome b_5 caused by the mutation from Val45 to Tyr45, His45 and Glu45. Compared with wild type (WT) cytochrome b_5, in all mutants the heme ring are CCW rotated relative to the imidazole planes of axial ligands and the angles β between two axial ligand imidazole planes are not changed, being in agreement with the temperature dependence of the shifts of the heme protons. The ratios of heme isomers (major to minor) are smaller than that in WT. The 4-vinyl group of the heme in V45Y assumes *cis*-orientation, being similar to that of WT, while in V45E and V45H, both *cis* and *trans* orientation are found. The relationships between the structure and biological function of the mutants are discussed in terms of the geometry of heme and axial ligands, the hydrophobicity of heme pocket and the electrostatic potential of the heme-exposed area.

Keywords: Cytochrome b_5/mutant V45E, V45H, V45Y/^{1}H NMR/structure-function relationship

1. Introduction

Cytochrome b_5 is a membrane-bound electron-transport protein. It functions as an electron carrier, participating in a series of electron-transfer processes in biological systems, including fatty acid denaturation [1–3], cytochrome P450 catalytic cycle, and the ferric methemoglobin reduction [4–6]. It contains heme with two histidines acting as its axial ligands. The His/His ligation rules out ligand binding in a physiological process and keeps its heme cycling between Fe^{2+} and Fe^{3+} forms. Cytochrome b_5 is one of the most extensively studied of the *b*-type cytochromes. It has become a model system for understanding structure–function relationships modulating electrochemical properties of *b*-type cytochromes.

To date, a number of studies concerning the influences of the orientation of the axial ligand plane on the spread and shift pattern of heme proton resonances and redox potential, as well as other spectroscopic properties using theoretical approach and model compounds have been reported [7,8]. In addition to extensive studies of the wild-type proteins, the site-directed mutagenesis has become an important tool for understanding cofactors to modulate the reduction potential and spectroscopic properties of bis-imidazole axially ligated heme proteins. However, to our knowledge, except the mutant A67V [9,10], no mutants have been successively designed to disturb the orientation of axial ligand plane, especially for axial ligand His39. In oxidized bovine microsomal wild type (WT) cytochrome b_5, Val45 is a highly conserved residue, which is a member of heme hydrophobic pocket residues (Fig. 1) [11]. It is very close to the heme edge and the axial ligand His39 imidazole plane. Therefore, the mutation at this site may cause perturbation on the orientation of the heme and the axial ligand plane and provide information on how the geometry of the axial ligands influences the

Abbreviations: CCW, Counter-clockwise; DSS, 2,2-dimethyl-2-silapentane-5-sulfonate; NMR, Nuclear magnetic resonance; NOE, Nuclear Overhauser effect; NOESY, Nuclear Overhauser effect spectroscopy; 1D, One-dimensional; TPPI, Time-proportional phase incrementation; 2D, Two-dimensional; WT, Wild type.

* Corresponding authors. Tel.: +86-21-6416-3300x1431; fax: +86-21-6416-6128 (H.W.); tel.: +86-21-6564-3973; fax: +86-21-6564-1740 (Z.-X.H.).
E-mail address: hmwu@mail.sioc.ac.cn (H. Wu).

doi:10.1016/j.biochi.2003.08.005

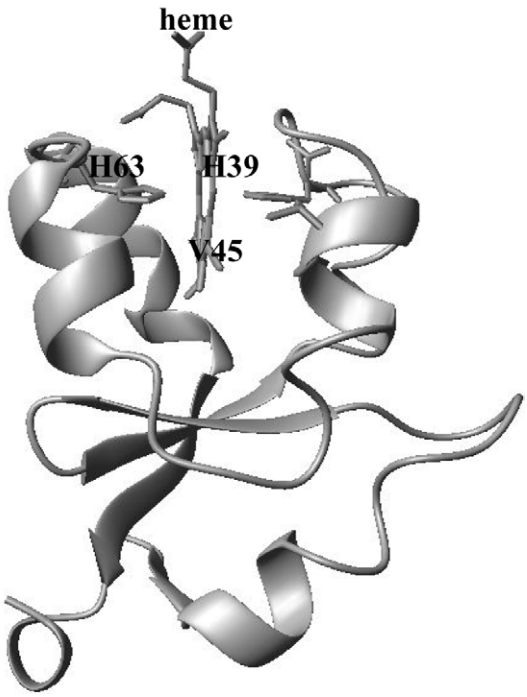

Fig. 1. Stereo-view of the Val45 in cytochrome b_5 using MOLMOL (pdb entry: 1EHB).

microenvironments of the heme pocket and the spectroscopic and electrochemical properties.

Three mutants were designed: the V45H and V45E were constructed to examine the effect of positive and negative charge on the stability and redox potential of the proteins, and the mutant V45Y was designed to introduce a bulkier residue with a hydroxyl group towards the heme pocket. All of these mutants have been characterized and their physical and electrochemical properties have also been reported [12]. The redox potentials of mutant V45Y, V45H, V45E and the WT cytochrome b_5 are –35, +8, –26 and –10 mV, respectively. And the stability of these mutants against heat and urea is lower than that of WT cytochrome b_5.

Compared with WT protein, UV–visible, CD and fluorescence spectroscopic studies showed that there was no marked change in the secondary structures of all mutants. Our previous proton NMR studies on the protein matrix of V45H mutant indicated that the global folding of the protein did not change, while the heme environment was disturbed by the mutation on Val45 [13]. Therefore, to investigate the effects of mutation at the residue Val45 on heme environment of cytochrome b_5 and the possible reasons which cause the variations in the redox potential and stability of the mutants, 1D and 2D ^{1}H NMR were employed to these mutants in this paper. The hyperfine-shifted signals of the heme protons were assigned unambiguously, and the chemical shifts were used to estimate variation of the orientation of the heme and the axial ligand planes. The 2D nuclear Overhauser effect spectroscopy (NOESY) spectrum was used to provide local conformational information on the hydrophobic pocket and heme itself. The temperature dependence of chemical shifts of heme methyl protons was employed to probe the change of electronic state of the variants. The relationships between the structure and biological function of the mutants were discussed in terms of geometry of heme and axial ligands, hydrophobicity of heme pocket and the electrostatic potential of the heme-exposed area.

2. Materials and methods

All chemicals used throughout were the best quality available. The three mutants of oxidized bovine microsomal cytochrome b_5 were prepared and characterized as previously described [12]. The sample deuteration for NMR experiments was performed by solvent exchange. The corresponding protein was firstly solved in deuterated 25 mM aqueous phosphate buffer whose pH was adjusted to around 7, maintained at room temperature for about 4 h, followed by lyophilization. This process was repeated at least twice for every protein. Lastly, the pH of NMR sample was regulated to 7 using DCl or NaOD, without correction for isotopic effect. The concentration of all NMR samples was between 2 and 3 mM.

All ^{1}H NMR spectra were acquired on Varian Unity Inova600 spectrometer operating at a proton Larmor frequency of 600.153 MHz. To investigate the temperature dependence of the hyperfine shifts of heme methyl protons, 1D ^{1}H NMR spectra were acquired at 278, 283, 288, 293, 298, 303, 308, and 313 K. To detect nuclear Overhauser effect (NOE) correlations among hyperfine-shifted signals, NOESY [14] experiments with a spectral width of about 60 ppm in both frequency dimensions, with recycle delay time of 100 ms and mixing time of 50 ms were recorded in a phase-sensitive mode. According to the stability of the mutants, the NOESY spectra for V45H and V45E were acquired at 293 K and for V45Y at 298 K. All 2D spectra data consist of 4096 data points in the acquisition dimension and of 1024 in the indirect dimension. Raw data were weighed with a phase-shifted squared sine bell window function, zero-filled and Fourier-transformed to obtain a final matrix of 4096 × 4096 data points. A polynomial base line correction was applied in both dimensions.

Quadrature detection was achieved by using time-proportional phase incrementation (TPPI) mode [14]. In all NMR experimental, pre-saturation sequence was used to suppress water peak. All NMR spectra were processed using the standard VNMR software package (VNMR 6.1B version) on a SUN Sparc station and analyzed on SGI Indigo II computer by XEASY program [15].

To obtain the values of the angle β between the two axial ligand imidazole planes and the angle ϕ between the bisector of the angle β and the metal–pyrrole II axis by non-linear curve fitting method with the program Origin6.0 (Microsoft), the chemical shifts of methyl group at 298 K were corrected by ±2.7 ppm for an average higher shift value of the protons of methyls 5 and 8, and an average lower shift value of the protons of methyls 1 and 3, respectively [16].

3. Results

3.1. Assignments of the heme protons

The downfield hyperfine shifted region of the 600-MHz ^{1}H NMR spectra of WT cytochrome b_5 and its mutants V45Y, V45H and V45E were shown in the Fig. 2. Apparently, the hyperfine shifts of the mutants are different from those of WT cytochrome b_5, and the heme signals of the mutants cannot be assigned directly on the basis of the similarity of the 1D ^{1}H NMR spectra between WT protein and its mutants. The complete assignment of heme protons was achieved on the basis of the unique NOE contacts between heme *meso*-Hs and methyls. Using the mutant V45H as an example, the assignments of heme protons were presented as followings: in the NOESY spectrum of V45H (Fig. 3), a *meso*-H signal at δ 10.35 uniquely showed NOE contacts with two methyl signals at δ 8.60 and 3.33, respectively. Therefore, the signal was assigned as δ-*meso*-H, and the methyl signals were 1- or 8-methyls. Using these signals as "entry points", a sequential NOE network between protons of vicinal heme substituents was identified. For example, the methyl signal at δ 8.60 was correlated to a vinyl proton signal at δ 23.22. Thus, the former was assigned as 1-methyl, and the latter was attributed to 2-vinyl H_α. In addition, the 2-vinyl-H_α showed NOE connection with a *meso*-H at δ –3.69, which in turn correlated to a methyl group at δ 17.16. Then the former was assigned as α-*meso*-H and the latter was 3-methyl group. The intact NOE network was demonstrated in Fig. 3 and the assignment results were summarized in Table 1. After finishing assignment of a complete set of heme protons, a number of signals with lower intensity and lack of scalar correlation was remained in this region. This fact suggested the presence of another heme isomer designated as minor isomer, while the former isomer was designated as major isomer. Among those signals, a *meso*-H at δ 7.80 solely correlated to a methyl signal at δ 21.48. The latter, in turn, showed NOE contacts with two protons of a propionate at δ 13.64 and 14.52. Therefore, these signals can be assigned as β-*meso*-H, 5-Me and 6-propionate H_αs of the minor isomer, respectively. Both 6-propionate H_α protons exhibited NOE contacts to a *meso*-H at δ –0.35, which was correlated to a propionate proton at δ 19.86. Thus, the former was assigned as γ-*meso*-H and the latter was 7-propionate H_α, respectively. At last, 7-propionate H_α was correlated to another 7-propionate H_α at δ 3.74, which in turn showed NOE contact to 8-Me signal at δ 27.47. The partial assignments of the minor isomer were also shown in Fig. 3 (the labels underlined) and remaining signals of the minor isomer were not assignable due to the hyperfine shifts and signal overlapping. The hyperfine shift signals of both heme-isomers of WT protein and other two mutants V45Y and V45E were assigned simultaneously in a similar manner, and the data were also listed in Table 1.

3.2. Heme orientation disorder

As presented above, in solution the WT cytochrome b_5 and its three mutants are mixtures of two inter-convertible heme isomers (i.e. heme orientation disorder) that differ by a 180° rotation of heme plane about the α, γ-*meso* axis of the heme (Fig. 4). When the heme protons were clearly assigned, the degree of heme orientation disorder (i.e. the ratio of two heme isomers) could be determined. Using the assignment in Table 1 as references, the ratio of heme isomers was calculated by comparison of 5-methyl signal integrity between the major and minor isomer. It was 4.3:1, 3.8:1 and 3.8:1 for V45H, V45Y and V45E, respectively. In this work, the heme

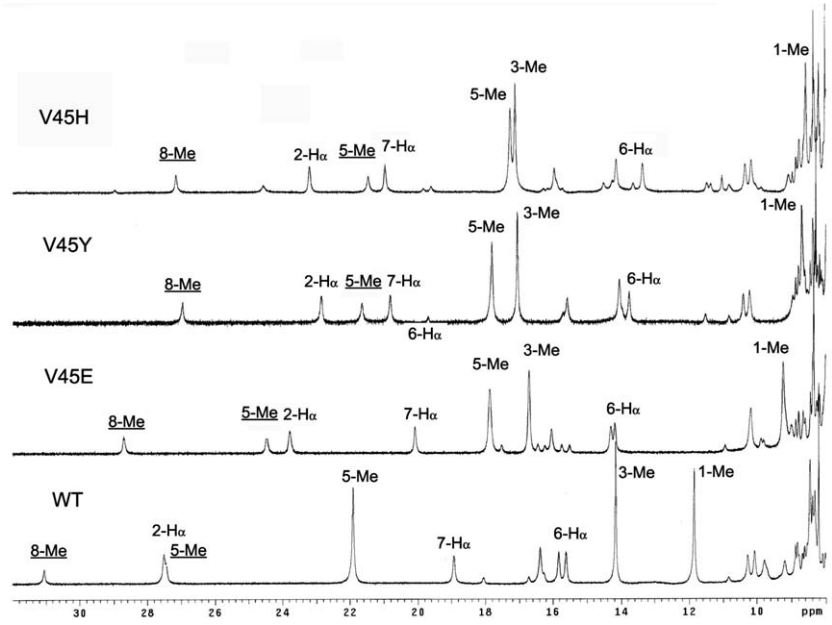

Fig. 2. The down-field shifted region of 1D ^{1}H NMR spectra of WT cytochrome b_5 and its mutants V45E, V45Y and V45H in D_2O, 25 mM phosphate buffer, pH 7.

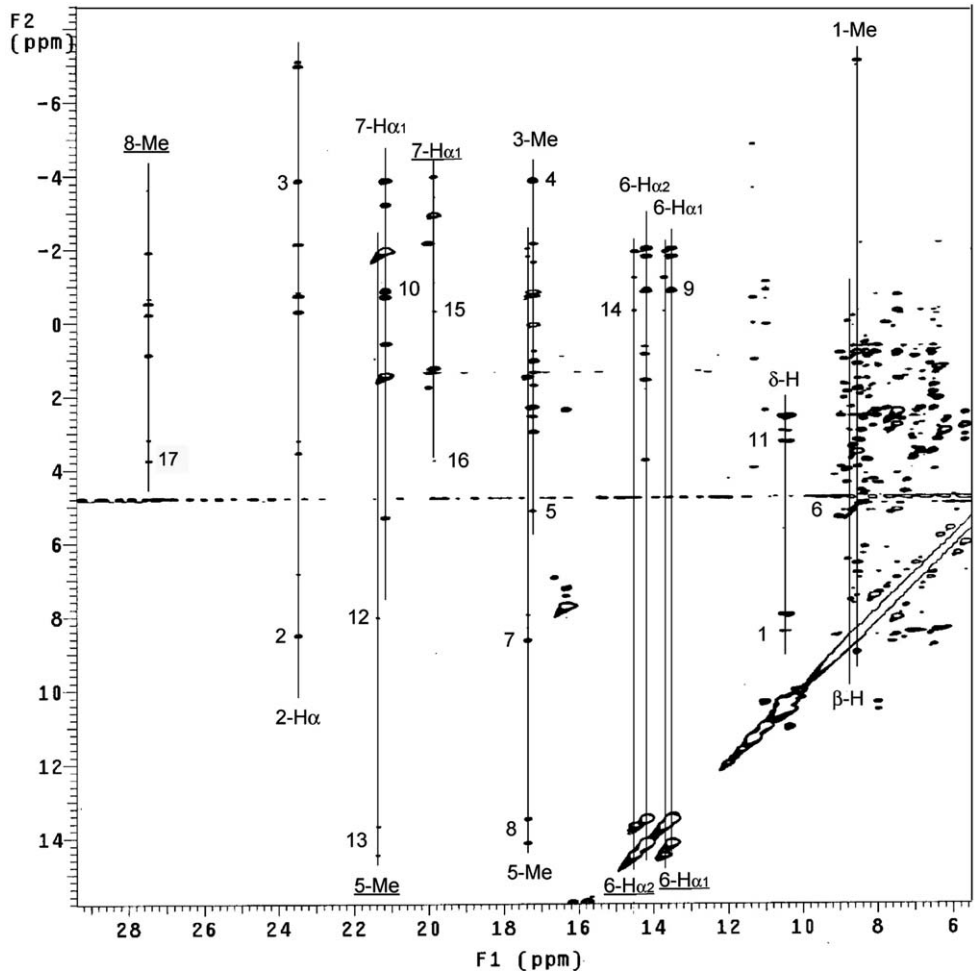

Fig. 3. The down-field shifted region of the NOESY spectrum of the mutants V45H in D_2O, 25 mM phosphate buffer, pH 7. The assignment without underline is for the major isomer, and the assignment with underline is for the minor isomer. The numbered peak was assigned for the pair of protons labeled in Fig. 4.

Table 1
Hyperfine shifts for WT cytochrome b_5 and its mutants V45E, V45Y and V45H, in 25 mM phosphate buffer, pH 7 and reference against DSS

Proton	Tb_5 (298 K)		V45E (298 K)		V45Y (298 K)		V45H (298 K)	
	Major isomer	Minor isomer	Major isomer	Minor isomer	Major isomer	Minor isomer	Major isomer	Minor isomer
1-Me	11.85		9.24		8.71		8.60	
2-H_α	27.50		23.79		22.87		23.22	
2-$H_{\beta\text{–t}}$	–7.21		–6.69		–6.87		–6.83	–7.88
2-$H_{\beta\text{–c}}$	–6.93		–6.48		–6.81		–6.76	–7.76
meso-H_α	–2.89	–2.44	–3.70		–3.50		–3.69	
3-Me	14.17	31.08	16.72		17.07		17.16	
4-H_α		18.05	5.35		5.23		5.14	
4-$H_{\beta\text{–t}}$	2.32		2.04		2.37		2.32	
meso-H_β	8.82	8.88	9.01		8.63	7.62	8.78	7.80
5-Me	21.91		17.87		17.82	21.66	17.30	21.48
6-α_1-H	15.82		14.30	14.35	14.06	14.06	14.16	14.52
6-α_2-H	15.61		14.19	14.24	13.77	14.06	13.3713.64	
meso-H_γ	–0.31		–0.45	–1.25	–0.45	–0.01	–0.52	–0.35
7-α_1-H	18.93	16.26	20.10	20.31	20.83	19.72	20.98	19.61
7-α_2-H	–1.82		–2.04		–1.75	3.75	–1.98	3.74
8-Me	2.70	27.46	3.33	24.75	3.34	26.99	3.33	27.16
meso-H_δ	9.77	8.55	10.17	8.49	10.21		10.35	

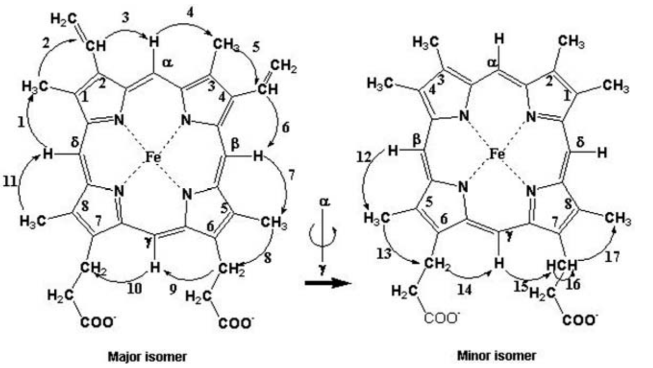

Fig. 4. Diagram of two heme orientation isomers. Two inter-convertible heme isomers differ by an 180° rotation of heme plane about its α, γ-*meso* axis. The arrows with number denote NOE contacts observed in Fig. 3.

isomer ratio in WT cytochrome b_5 was 6.5:1, which is almost identical to the previous reported (6.8:1) [17].

3.3. NOE correlations between heme protons and protons of surrounding residues

To probe the heme orientation of the major isomer, the NOE contacts among the heme protons of major isomer and some particular residues around the heme pocket were identified in the NOESY spectrum. These residues are Leu23, Leu25, Tyr30, Leu32, Phe35, Leu46, Ala54, Phe58, Ala67, Leu70, Ser71 and Phe74, and the identified NOE contacts were listed in Table 2.

The heme orientation of the major isomer was indicated by NOE contacts between relevant heme proton and protons of specific amino acid of peripheral protein matrix. As shown in Table 2, almost same NOE contacts array between the heme methyl of major isomer and protons of particular amino acid residues were observed for WT type b_5 and its three mutants. This fact clearly indicated that the heme orientation of the major isomer in these mutants is the same to that of WT cytochrome b_5 in the solution. In this paper, we focus on the discussion about the major heme isomer of WT cytochrome b_5 and its three mutants.

3.4. Temperature dependence of hyperfine shifts of heme protons

For paramagnetic systems, the temperature dependence of hyperfine shifts of the heme protons was usually presented by Curie plot (observed shift vs. reciprocal absolute temperature). In the special case of a well-isolated spin state with no zero-field splitting (ZFS), the diagonal paramagnetic susceptibility tensor χ obeys the Curie law, and hence both δ_{con} and δ_{dip} will exhibit strict Curie behavior (linear in $1/T$ with zero intercept at $T \rightarrow \infty$). For the present systems, the Curie plots of temperature dependence of hyperfine shifts for the heme methyls of WT cytochrome b_5 and its V45H, V45E and V45Y mutants in the region of 278–313 K were shown in Fig. 5.

4. Discussion

4.1. The heme geometry and orientation of axial ligands plane in the mutants

In general, the hyperfine shifts of heme protons contain a wealth of information on the structure, electronic and magnetic properties in hemoproteins. As shown in Table 1, the chemical shifts of the heme protons in the mutant proteins significantly changed in comparison with those of WT cytochrome b_5. This indicated that the heme geometry and the orientation of axial ligands plane in the mutants was perturbed by the site-directed mutation on Val45.

La Mar and coworkers have shown that the heme rotated about His–Fe–His axis in order to accommodate variations in the polypeptide, and the heme hyperfine shifts variations can be taken as indicators of this kind rotation in hemoferric proteins [18]. The rotation of heme relative to the axial His plane follows a well-defined relationship: if 1-CH_3, 5-CH_3

Table 2
NOE correlation observed among the protons of major heme isomer and residues around the hydrophobic pocket of WT cytochrome b_5 and its three mutants, in 25 mM phosphate buffer, pH 7

Heme proton	Protons of the residues around hydrophobic pocket			
	Tb_5 (293 K)	V45Y (298 K)	V45H (293 K)	V45E (293 K)
1-Me	Leu^{32} $H_{1\text{-Me}}$, Phe^{35} H_ζ, Phe^{58} H_ε, Leu^{70} H_α,H_β, H_γ, $H_{1\text{-Me}}$, $H_{2\text{-Me}}$, Ser^{71} H_N, H_α, H_β, Phe^{74} H_δ, H_ε, H_ζ	Tyr^{30} H_δ, H_ε, Leu^{32} $H_{1\text{-Me}}$, Phe^{35} H_ζ, H_δ, Phe^{58} H_ε, Leu^{70} H_α, H_β, H_γ, $H_{1\text{-Me}}$ $H_{2\text{-Me}}$, Ser^{71} H_β, Phe^{74} H_β, H_δ, H_ε, H_ζ	Tyr^{30} H_δ, Phe^{35} H_δ, H_ζ, Leu^{70} H_α, H_β, H_γ, $H_{1\text{-Me}}$, $H_{2\text{-Me}}$, Ser^{71} H_β, Phe^{74} H_β, H_δ, H_ε	Tyr^{30} H_δ, Phe^{35} H_ζ, H_δ, Leu^{70} H_α, H_β, H_γ, $H_{1\text{-Me}}$ $H_{2\text{-Me}}$ Ser^{71} H_N, H_α, H_β, Phe^{74} H_β, H_ζ
3-Me	Leu^{23} $H_{2\text{-Me}}$, Leu^{25} $H_{1\text{-Me}}$ $H_{2\text{-Me}}$, Leu^{46} H_γ, Ala^{54} H_β	Leu^{23} $H_{2\text{-Me}}$ $H_{1\text{-Me}}$, Leu^{25} $H_{1\text{-Me}}$ $H_{2\text{-Me}}$, Ala^{54} H_β	Leu^{23} $H_{2\text{-Me}}$ $H_{1\text{-Me}}$, Leu^{25} $H_{1\text{-Me}}$ $H_{2\text{-Me}}$, Ala^{54} H_β	Leu^{23} $H_{2\text{-Me}}$ $H_{1\text{-Me}}$, Leu^{25} $H_{1\text{-Me}}$ $H_{2\text{-Me}}$, Ala^{54} H_β
5-Me	Val^{45} $H_{\gamma 1\text{-me}}$, $H_{\gamma 2\text{-Me}}$	Tyr^{45} H_δ, H_ε	His^{45} H_δ, H_ε	Glu^{45} H_γ
8-Me	Ala^{67} H_α, Leu^{70} $H_{1\text{-Me}}$	Ala^{67} H_α, Leu^{70} $H_{1\text{-Me}}$	Ala^{67} H_α, Leu^{70} $H_{1\text{-Me}}$	Ala^{67} H_α Leu^{70}, $H_{1\text{-Me}}$
2-vinyl$H_{\beta\text{–t}}$	Leu^{25} $H_{2\text{-Me}}$, Leu^{32} $H_{1\text{-Me}}$, Ser^{71} H_α, H_β, Phe^{74} H_β, H_δ	Leu^{25} $H_{2\text{-Me}}$, Tyr^{30} H_δ, H_ε, Leu^{32} $H_{1\text{-Me}}$, Ser^{71} H_β, Phe^{74} H_β, H_δ	Leu^{25} $H_{2\text{-Me}}$, Tyr^{30} H_δ, H_ε, Leu^{32} $H_{1\text{-Me}}$, Ser^{71} H_β, Phe^{74} H_β, H_δ	Leu^{25} $H_{2\text{-Me}}$, Tyr^{30} H_δ, H_ε, Leu^{32} $H_{1\text{-Me}}$, Ser^{71} H_β, Phe^{74} H_β, H_δ
2-vinyl $H_{\beta\text{–C}}$	Leu^{23} $H_{2\text{-Me}}$, Leu^{25} $H_{2\text{-Me}}$, Tyr^{30} H_δ, H_ε, Leu^{32} $H_{1\text{-Me}}$, Ser^{71} H_α, H_β, Phe^{74} H_β, H_δ	Leu^{23} $H_{2\text{-Me}}$, Leu^{25} $H_{2\text{-Me}}$, Tyr^{30} H_δ, H_ε, Leu^{32} $H_{1\text{-Me}}$, Ser^{71} H_β, Phe^{74} H_β	Leu^{23} $H_{2\text{-Me}}$, Leu^{25} $H_{2\text{-Me}}$, Tyr^{30} H_δ, H_ε, Ser^{71} H_β, Phe^{74} H_ε	Leu^{25} $H_{2\text{-Me}}$, Tyr^{30} H_δ, H_ε, Leu^{32} $H_{1\text{-Me}}$, Ser^{71} H_β, Phe^{74} H_β, H_δ
2-vinyl H_α	Leu^{25} $H_{2\text{-Me}}$, Leu^{32} $H_{1\text{-Me}}$, Ser^{71} H_α, H_β, Phe^{74} H_δ	Leu^{25} $H_{2\text{-Me}}$, Leu^{32} $H_{1\text{-Me}}$, Ser^{71} H_α, Phe^{74} H_δ, H_β	Leu^{25} $H_{2\text{-Me}}$, Leu^{32} $H_{1\text{-Me}}$, Ser^{71} H_β, Phe^{74} H_δ	Leu^{25} $H_{2\text{-Me}}$, Leu^{32} $H_{1\text{-Me}}$, Phe^{74} H_δ

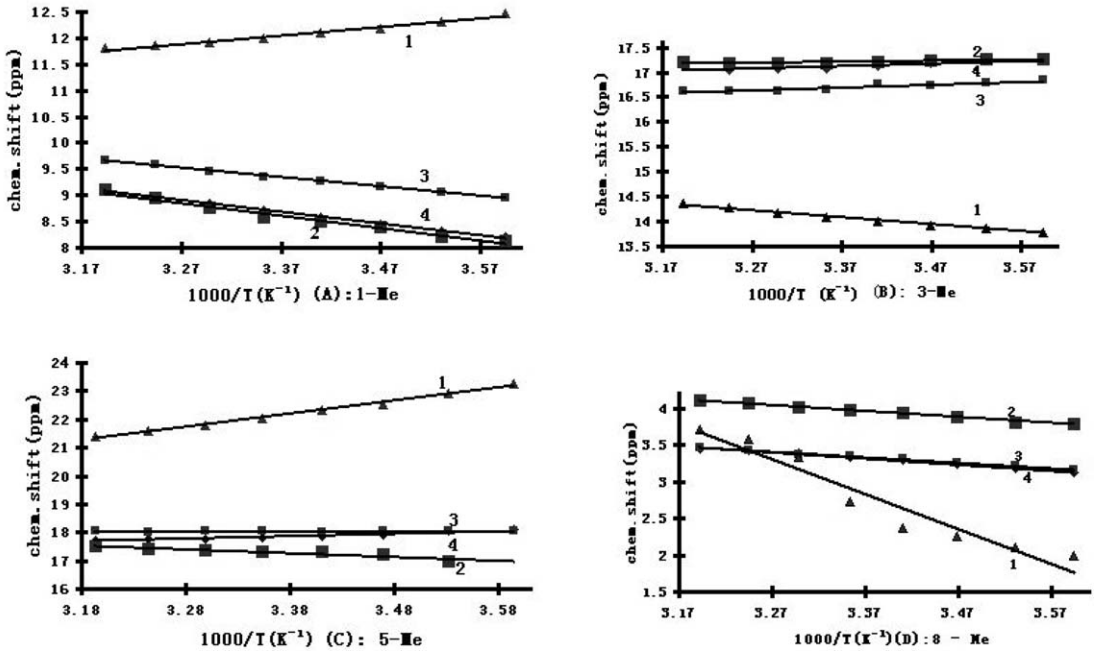

Fig. 5. The Curie plots of the temperature dependence of hyperfine shifts of the heme protons for WT cytochrome b_5 and its mutants. The curves with label 1–4 is for WT b_5 and its mutants V45H, V45E and V45Y, respectively.

and *meso*-H_α, *meso*-H_γ move to upfield, 3-CH_3, 8-CH_3 and *meso*-H_β, *meso*-H_δ, must move to downfield. In other words, if the methyl shift spread increases (decreases), the *meso*-H shift spread must decrease (increase).

From the data of the hyperfine shifts of the major isomer of the mutants shown in Table 1, it is obvious that 1-CH_3, 5-CH_3, *meso*-H_α and *meso*-H_γ move to upfield, while 3-CH_3, 8-CH_3 *meso*-H_β and *meso*-H_δ, except the *meso*-H_β of V45H and V45Y (it will be discussed later), move to downfield compared with those of WT cytochrome b_5. In addition, the spreads of heme methyl shifts of the mutants (13.97, 14.48 and 14.54 ppm for V45H, V45Y and V45E, respectively) are smaller than that of the WT cytochrome b_5 (19.21 ppm). While the spreads of heme *meso*-Hs shift in the mutants (14.04, 13.71, and 13.67 ppm for V45H, V45Y and V45E, respectively) are larger than that of WT cytochrome b_5 (12.66 ppm). Therefore, it can be concluded that a heme rotation relative to the imidazole plane of axial ligand, His39 occurred upon the mutation on Val45.

According to La Mar's interpretation [18], the variation of the spread of the *α, γ-meso*-H to *β, δ-meso*-H shifts as a function of the heme rotation angle ψ, changes at a rate of approximate 0.2 ppm per ° in the interesting region (ψ approximately 15°) of cytochrome b_5. The mean *α, γ-meso*-H to *β, δ-meso*-H spread (defined as *Δmeso*), are 11.67, 11.42, 11.67 and 10.90 ppm for V45H, V45Y, V45E and WT, respectively. Therefore, the increase in *Δmeso* of 0.77, 0.52, and 0.77 ppm of mutant V45H, V45Y and V45E versus WT indicated a counter-clockwise (CCW) rotation of approximately 3.3°, 2.6° and 3.3°, respectively.

On the other hand, Walker and coworkers found that the predicted heme methyl and *meso*-H shifts by simple Huckel calculations of the effect of the axial ligand nodal plane orientation on the contact shifts are consistent with the observed methyl shifts of a large number of heme proteins [19]. In addition, Bertini and his coworkers pointed out that in bis-histidine system the hyperfine shifts of the methyl protons are related to the angle ϕ between the Fe–N(2) axes and the bisector of the acute angle β between the two histidine planes, as well as the angle β itself, and further proposed a heuristic equation (Eq. 1) to correlate these factors [16]:

$$\delta_i = \cos\beta\,[a\sin^2(\theta_i - \phi) + b\cos^2(\theta_i + \phi) + c] + d\sin\beta \quad (1)$$

Herein, θ_i is the angle between the metal–*i*th–methyl direction and the metal–pyrrole II axis. For the systems of cytochrome b_5, the parameters a = 38.8 ± 1.4 ppm, b = –10.5 ± 1.0 ppm, c = –1.1 ± 0.8 ppm and d = 9.4 ± 0.6 ppm. Therefore, it was able to calculate the angles β and ϕ for the present mutants using observed chemical shifts of heme methyls of these proteins through non-linear curve fitting method and the results were listed in Table 3. It was clear that, the angle ϕ of mutant V45E, V45H and V45Y is smaller than that of the WT by about 3°, indicating the heme CCW rotation about 3° relative to the mean plane of two axial ligands in these mutants. The values of heme rotation in these mutants are in agreement with those (ψ) estimated from the chemical shifts of the *meso*-Hs within experimental error.

The heme rotation about its normal should be reflected by the NOE contacts observed between the heme protons and the surrounding residues in hydrophobic pocket. However, the data in Table 2 indicated that there were little difference between the WT and its mutants. Consequently, at the present stage it is not clear that the changes in ϕ angles should be attributed to the heme rotation around its normal or to the variation of imidazol plane of the axial ligands, which is

Table 3
The comparison between WT b_5 and its mutants in the heme isomer ratio, hyperfine shifts of the heme protons and the geometry of the heme and axial ligand planes, which are correlated with the change of neat charge, the volume and hydrophobic free energy of side-chains of substituted residues

	WT b_5	V45Y	V45H	V45E
Isomer ratio	6.5:1	3.8:1	4.3:1	3.8:1
Charge of 45th res.	0	0	+1	–1
Volume of 45th res. ($Å^3$)[27]	0	+62	+26	+13
Hydrophobicity (kJ mol^{-1})	0	+0.4	–1.6	–2.7
Δmeso (ppm) in 298 K	10.86	11.38	11.68	12.12
Average δ of methyl	12.65	11.73	11.60	11.79
Average δ of *meso*-H	4.01	3.71	3.71	3.69
2-vinyl (in isomer A)	*cis/trans*	*cis/trans*	*cis/trans*	*cis/trans*
4-vinyl (in isomer A)	*cis*	*cis*	*cis/trans*	*cis/trans*
Ψ (°)	–	2.6	3.3	3.3
Φ (°)	148.62 ± 0.37	145.33 ± 0.33	145.34 ± 0.29	145.32 ± 0.36
β (°)	13.64 ± 0.42	13.52 ± 0.42	13.50 ± 0.42	13.56 ± 0.43

$\Delta meso = 0.5(\delta_{\beta H} + \delta_{\delta H} - \delta_{\alpha H} - \delta_{\gamma H})$.

waiting for the three dimensional structure study on these mutants.

4.2. Influence of mutation on the heme orientation disorder

As shown above, the ratios of heme isomers in the mutants became smaller in comparison with that of WT. Thus, it is worth considering why the replacement of conservative residue Val 45 with Tyr, His and Glu resulted in this variation in the heme isomer ratios of the proteins. It has been reported that three native ferricytochrome b_5 from rat, beef and chicken exhibit variable degrees of heme orientation disorder, with the equilibrium constant of 1.6, 8.9 and 20, respectively [20]. In this case, the heme orientation disorder has been attributed to the van der Waals contacts between the heme 2-vinyl group and the hydrophobic cluster consisted by residues 23, 25 and 32 in these proteins.

For the present systems, the van der Waals contact was firstly considered. In the X-ray structure of WT protein, Val45 is very close to the heme edge and the side chain of residue Val45 is towards *meso*-H_β. Thus, it probably makes van der Waals contacts with *meso*-C_β and nearby 4-vinyl group in WT protein. This was evidenced by abnormal high-field shifts of the *β-meso*-H in the mutant V45Y and V45H versus mutant V45E. As mentioned in previous section, the changes of *β-meso*-H shifts of the mutants V45Y and V45H deviated from the trends reported by La Mar, for which the shielding effect by the aromatic ring of the 45th residues side-chains in these mutants should be a rational explanation.

Consideration of space arrangement of the heme substitute groups in these heme isomers, the position of heme 4-vinyl will be displaced by heme 1-CH_3 upon the heme ring rotating over 180° along its α, γ-axis. The volume of vinyl group is larger than that of methyl. The hindrance between 4-vinyl and the side-chain of 45th residue is larger than that between 1-methyl and the side-chain of 45th residue due to van der Waals repulsion. The volume of the side-chain of 45th in the mutants, as listed in Table 3, is larger than that of WT cytochrome b_5 [21]. Therefore, the lower heme isomer ratio of the mutants than that of WT protein is likely reasonable. Among these mutants, the volume of the side-chain of Tyr45 is the largest. Hence, the steric hindrance of side-chain of Tyr45 to the heme moiety is the largest and its heme isomer ratio should be the smallest among the mutants.

On the other hand, the mutant V45E and V45H showed unusual behavior: the mutant V45H exhibited biggest heme isomer ratio, while V45E was the same with V45Y, which can not be simply accounted for by their different volume of the residue 45. Actually, these two mutants can be differentiated by their electrostatic property: mutant V45H possesses positive charge, while mutant V45E is negatively charged. The heme 4-vinyl is an electron-rich group due to its electron-drawing ability (refer to latter discussion). Therefore, the interaction between the side chain of residue 45 and 4-vinyl group of the heme in major isomer for V45H and V45E were different: attractive for V45H and repulsive for V45E, respectively. Clearly, it was favorable for the major isomer of mutant V45H over that of V45E.

4.3. Orientation of the heme vinyl groups in the mutants

The orientations of both 2- and 4-vinyl groups of the heme have been invoked to explain the reduction properties of cytochrome b_5. Heme proteins can affect the redox potentials of their heme reduction centers by constraining the position of vinyl groups with respect to the plane of the heme and thereby affecting the electron-drawing ability of the vinyl groups. When the vinyl groups align with the plane of the heme, their electron-drawing ability is enhanced and the redox potential of the heme center is increased [22,23].

Four combinations of vinyl group orientation of the heme were represented in Fig. 6. In general, NOE contacts observed between 1-Me/2-vinyl $H_{\beta-t}$ and 1-Me/2-vinyl H_α protons indicate the presence of *cis* and *trans* orientations of 2-vinyl group. Solely NOE between 3-Me/4-vinyl $H_{\beta-t}$ and between *β-meso*-H/4-vinyl H_α infers that there is only *cis* orientation of 4-vinyl group. In present systems, observed NOE contacts showed that 2-vinyl group of the major heme

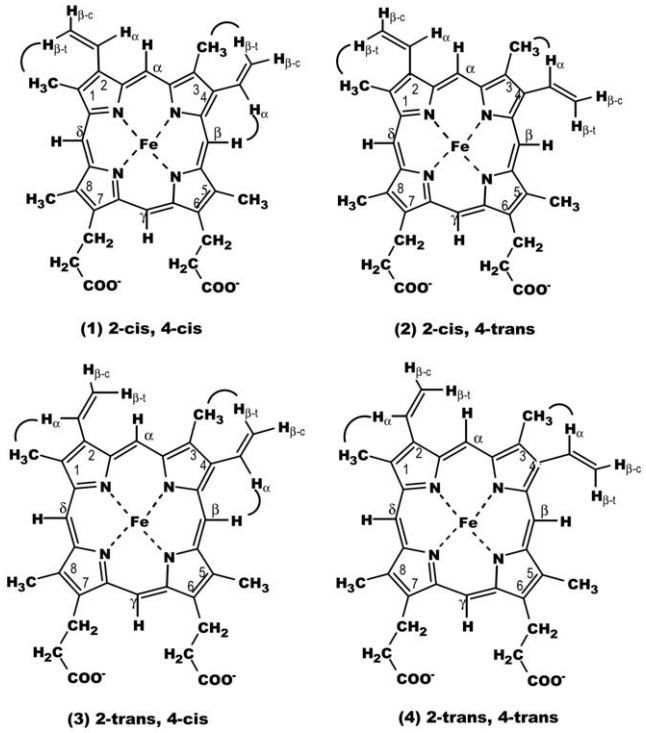

Fig. 6. The possible orientation of 2-vinyl and 4-vinyl in heme of cytochrome b_5. The curves denote the NOE contacts observed between relevant heme methyl protons and vinyl protons.

isomer of WT cytochrome b_5 and its three mutants interconverted rapidly on NMR time scale between *cis* and *trans* orientations (Table 2). In WT and V45Y, NOE observations showed that orientation of 4-vinyl group was *cis*, the same as the reported [17]. However, in mutant V45E and V45H, besides the NOE contacts between 3-Me/4-vinyl $H_{\beta-t}$ and NOE between *meso*-H_β/4-vinyl H_α, a weaker NOE peak between 3-Me and 4-vinyl H_α was also observed. This fact indicated that besides *cis* orientation, the *trans* orientation of 4-vinyl group existed to some extent. Why did this kind of orientation change occur in the mutant V45H and V45E?

As pointed out previously, the residue Val45 is a part of the heme hydrophobic pocket and the relative hydrophobicity of the mutating residue must be considered. For mutant V45H and V45E, the side-chains having positive and negative charge may move away from the heme center due to their higher hydrophilicity, and extend to the edge of the heme pocket to avoid the decrease of hydrophobic free energy of heme pocket. This variance in the orientation of the side chain in these mutants may decrease the steric hindrance between 4-vinyl group and the side chain of residue-45, and thus both *cis* and *trans* configuration of heme 4-vinyl group occurred. For WT and V45Y, the binding between the heme moiety and the heme hydrophobic pocket are tighter, due to the higher hydrophobicity of their side chains, than that of V45H and V45E. Therefore, the rotation of 4-vinyl in WT and V45Y may be restricted, and only the *cis* configuration of heme 4-vinyl group existed.

4.4. Temperature dependence of NMR hyperfine-shifted signals of the mutants

As shown in Fig. 5, it was clear that the temperature dependence of the hyperfine shift of the heme methyl protons of the mutants was not identical with those of WT cytochrome b_5. For WT cytochrome b_5, 1-CH_3 and 5-CH_3 exhibited hypo-Curie behavior, while 3-CH_3 and 8-CH_3 showed anti-Curie type behavior, which follow the general way: the lowest-field methyl exhibits the stronger hyper-Curie behavior and the highest-field methyl exhibits the stronger hypo-(to anti-)Curie behavior. For the three mutants, the temperature behavior of 1-CH_3 group changed from hypo-Curie to anti-Curie as the chemical shifts moving to higher field, while 3-CH_3 of the heme changed from anti-Curie to hypo-Curie as their chemical shifts moving to lower field. The temperature dependence of 5-CH_3 of the mutants also changed from hypo-Curie to non-Curie (V45E and V45Y) or anti-Curie (V45H) as their chemical shifts moving to higher field. The 8-CH_3 groups of the mutants still showed anti-Curie behavior as their chemical shifts only slightly low-field shifting, and the absolute values of the Curie factors are much less than that of WT cytochrome b_5.

For a well-defined electronic ground state, interpretation of the temperature dependence will depend on the electron structure of the protein. The temperature dependence of hyperfine shifts is related to the energy separation between the ground and the excited states, which, in turn, is modulated by interactions between the iron and axial ligands [24]. In other wards, the temperature dependence of the heme proton shifts gives an indication of the splitting of the d_{xz}, d_{yz} orbitals and thus contains information on the heme geometry and dihedral angle between the two π bounding axial ligands.

The difference in temperature dependence of the hyperfine shifts between the mutants and WT protein indicated that the interaction between the iron and the axial ligands in the mutants was influenced and the electron structure of the Fe(III) d_π orbital was changed due to the mutation on Val45. In previous section, the values of dihedral angle β between two axial ligands calculated according to Eq. 1 (see Table 3) for WT cytochrome b_5 and its mutants are almost same. Therefore, the differences in the Curie behavior of temperature dependence of heme methyls may be attributed to the heme rotation relative to the nodal plane of the axial ligand.

It has been pointed out that the orientation of the axial ligand planes with respect to heme (i.e. the angle ϕ) determines the energy difference between two anti-bond e (π) orbitals of heme ring [7]. The odd-number electron in higher energy orbital spin delocalization leads to the change of the spin density of heme ring. The latter is correlated to the average chemical shifts of the heme methyl and *meso*-H. The averaged chemical shifts of heme methyl and *meso*-H in the mutants as shown in Table 3 were smaller than those of WT cytochrome b_5, indicating that the averaged electron spin density of heme ring in the mutants is lower than that in WT

cytochrome b_5. Therefore, the decrease in the average chemical shifts of methyl and *meso*-Hs are consistent with the angle ϕ.

4.5. Factors regulating the redox potential of the mutants

Factors regulating the redox potential of the hemoproteins are well-addressed topics in the literature. It has been correlated to geometry of the axial ligand planes, orientation of heme vinyl groups, orientation of the extended propionate, heme rotation around its normal, heme orientation disorder, and electrostatic potential around the heme-exposed area, as well as hydrophobicity of the heme pocket. (1) Walker and his coworkers reported that the perpendicular alignment of planar axial ligands could lead to a positive shift in redox potential of up to about 50 mV over that observed for parallel alignment, when all other structural and environmental factors being equal [6,7]. (2) As mentioned above, the orientations of heme vinyls also affect the redox potential of heme protein: when the vinyl groups align with the plane of the heme, their electron-drawing ability is enhanced and the redox potential of the heme center is increased [22,23]. (3) La Mar and his coworkers have shown that the redox potential becomes more negative for an axial histidine imidazole plane that is parallel to the N–Fe–N vector rather than bisecting the two N–Fe–N vectors. The heme rotation CCW about the His–Fe–His bond would decrease the angle between His39 imidazole plane and N_A–Fe–N_C vector consistent with a more negative redox potential [17]. (4) The angular accommodation of the heme due to a protein perturbation also likely influence the orientation of the extended propionate, which participates in a salt-bridge in 'docking' with its reduction partner [25]. (5) The heme orientation disorder has influence in the redox potential of cytochrome b_5, because the heme rotation 180° about α, γ-*meso* axis would also decrease the angle between His39 imidazole plane and the N_A–Fe–N_C vector. It has previously been reported that in beef cytochrome b_5 the major and minor isomer exhibits the redox potential of 0.8 and –26.2 mV, respectively [26]. (6) The decrease of the hydrophobicity of the heme pocket, which can be resulted not only from the change of residue properties, but also from the variance of H-bond network and water molecule, makes the protein redox potential more negative [27]. (7) The electrostatic potential around the heme-exposed area regulates the redox potential of the protein: the increase of positive (negative) charge at the heme exposed surface always make the redox potential shift positively (negatively), due to stabilizing (destabilizing) reduced state of the heme iron ion [28,29].

In present system, the observed redox potential of V45Y (–35 mV), V45H (+8 mV) and V45E (–26 mV) were distinctly different from that (–10 mV) of WT protein. The influences of the factors mentioned above on the redox potential of the mutants can be estimated as followings: (1) The calculated dihedral angles β between two axial ligands in WT protein and three mutants are almost same, and its influence on the redox potential can be ignored. (2) The presences of *trans* orientation of 4-vinyl group in the solution of V45E and V45H mutants infer the lower coplanity of 4-vinyl, which may move their redox potential negatively. (3) The angles ϕ between the Fe–N(2) axes and the average axial histidine ring plane in the mutants became smaller than that of WT cytochrome b_5, which may lead to negatively moving of the redox potential. (4) The orientation of propionates and its influence on the redox potential of the mutants currently are unknown in this system. (5) The heme orientation disorder ratio (major to minor) of the mutants become lower than that of WT cytochrome b_5. The increase of heme isomer B concentration in the solution of the mutants may move the redox potential negatively. (6) The decrease of hydrophobicity of heme pocket due to positive or negative charge and polar group of the 45th residues in the mutants may move the redox potential more negatively. For the mutant V45Y, the variance of the redox potential may be attributed to the coordinate action of all factors above. However, for mutant V45H and V45E, the electrostatic potential around the heme-exposed area should be dominant: in V45H, the increase of positive charge density in heme-exposed area moved redox potential positively, while in V45E, the increase of negative charge density moved the redox potential negatively.

4.6. Factors on the stability of the mutants

Several factors, including the hydrophobic effect, hydrogen bond, salt bridge, and van der Waals contacts contribute to the stability of the protein. Among these, hydrophobic interaction is considered to be dominant. It was reported that the hydrophobic effects contribute approximately 8 kJ mol^{-1} per residue, on the average, to the free energy of the protein folding at room temperature [21]. In this study, the stability of the mutants and WT cytochrome b_5 against heat and urea was in order of WT > V45Y ~ V45H > V45E. As mentioned above, the hydrophobic interaction between the heme and protein matrix was decreased due to the introduction of polar group and positive or negative charges on 45th residues. Therefore, the binding between the heme and the protein pocket became weaker after the mutation on Val45, which resulted in the decrease of the stability of the mutants against heat and urea.

5. Conclusion

The results obtained in this study provided further insight into the importance of the residue Val45 in cytochrome b_5. Val45 is a conserved residue and locates close to the edge of heme in the heme pocket. The variations in structure and function of the mutants are closely related to the properties of the side-chain of 45th residues, such as the volume, the electrostatic charge, as well as the hydrophobicity. The mutation at Val45 gives influences on various aspects of the structure and property of the mutants: including the heme

geometry and the orientation of axial ligands, the heme isomer ratio, the orientation of heme vinyl group, and further on the stability and redox potential of the mutants. All these results reflect the subtlety of prosthetic group–protein interactions in cytochrome b_5.

Acknowledgements

This project was supported by the National Science Foundation of China (No. 20132030), Chinese Academy of Sciences, and State Minister of Science and Technology of China. The authors are indebted to Professor A.G. Mauk of University of British Columbia, Canada, for his kind gifts of cytochrome b_5 gene; to the Institute of Molecular biology and Biophysics, ETH-Hönggerberg Zürich, Switzerland, for the program XEASY.

References

[1] P. Strittmatter, S.F. Velick, J. Biol. Chem. 228 (1957) 785–789.
[2] N. Oshino, Y. Imai, R. Sato, J. Biochem. (Tokyo) 69 (1971) 155–162.
[3] T. Kajihara, B. Hagihara, J. Biochem. (Tokyo) 63 (1968) 453–481.
[4] D.E. Hultquist, P.G. Passon, Nature (London) New. Biol. 229 (1971) 252–253.
[5] K. Abe, Y. Sugita, Eur. J. Biochem. 101 (1979) 423–428.
[6] M. Nakai, T. Yubisui, Y. Yoneyama, J. Biol. Chem. 255 (1980) 4599–4602.
[7] F.A. Walker, B.H. Huynh, W.R. Scheidt, S.R. Osvath, J. Am. Chem. Soc. 108 (1986) 5288–5297.
[8] Z.R. Korsun, F. Moffat, K. Frank, M.A. Cusanovich, Biochemistry 21 (9) (1982) 2253–2258.
[9] S. Sarma, B. Dangi, C. Yan, R.J. Digate, D.L. Banville, R.D. Guiles, Biochemistry 36 (19) (1997) 5645–5657.
[10] S. Sarma, R.J. Digate, D.B. Goodin, C.J. Miller, R.D. Guiles, Biochemistry 36 (19) (1997) 5658–5668.
[11] J. Wu, J.H. Gan, Z.X. Xia, Y.H. Wang, W.H. Wang, L.L. Xue, et al., Proteins: struct. funct. genet. 40 (2) (2000) 249–257.
[12] Z.Q. Wang, Y.H. Wang, W.H. Wang, L.L. Xue, X.Z. Wu, Y. Xie, et al., Biophys. Chem. 83 (1) (2000) 3–17.
[13] C.Y. Cao, N.X. Zhang, Y.F. Wang, H.M. Wu, Z.Q. Wang, Y.H. Wang, et al., Acta Chim. Sin. 59 (4) (2001) 578–586.
[14] D. Marion, K. Wuthrich, Biochem. Biophys. Res. Commun. 113 (1983) 967–974.
[15] C. Eccles, P. Güntert, M. Billeter, K. Wüthrich, J. Biomol. NMR 1 (1991) 111–130.
[16] I. Bertini, C. Luchinat, G. Parigi, F.A. Walker, J. Biol. Inorg. Chem. 4 (1999) 515–519.
[17] K.B. Lee, E. Jun, G.N. La Mar, I.N. Rezzano, R.K. Pandey, K.M. Smith, et al., J. Am. Chem. Soc. 113 (9) (1991) 3576–3583.
[18] K.B. Lee, G.N. La Mar, K.E. Mansfield, K.M. Smith, T.C. Pochapsky, S.G. Sligar, Biochim. Biophys. Acta 1202 (1993) 189–199.
[19] N.V. Shokhirev, F.A. Walker, J. Biol. Inorg. Chem. 3 (6) (1998) 581–594.
[20] K.B. Lee, G.N. La Mar, L.A. Kehres, E.M. Fujinari, Biochemistry 29 (41) (1990) 9623–9631.
[21] M.S. Caffrey, Strategies for the study of cytochrome *c* structure and function by site-directed mutagenesis, Biochimie 76 (1994) 622–630.
[22] L.S. Reid, A.R. Lim, A.G. Mank, J. Am. Chem. Soc. 108 (1986) 8197–8201.
[23] L.S. Reid, R. Marcia, A.G. Mauk, J. Am. Chem. Soc. 106 (1984) 2182–2185.
[24] K.L. Bren, H.B. Gray, L. Banci, I. Bertini, P. Turano, J. Am. Chem. Soc. 117 (1995) 8067–8073.
[25] F.R. Salemme, J. Mol. Biol. 102 (1976) 563–568.
[26] F.A. Walker, D. Emrick, J.E. Rivera, B.J. Hanquet, D.H. Buttlaire, J. Am. Chem. Soc. 110 (1988) 6234–6240.
[27] P. Yao, X.H. Wang, Y.L. Sun, Z.X. Huang, Y. Xie, G.T. Xiao, et al., Protein Eng. 10 (6) (1997) 575–581.
[28] F. Mathews, E. Czerwinski, in: A. Martonosi (Ed.), The enzymes of biological membranes, Wiley, New York, 1976, pp. 143–147.
[29] M.S. Caffrey, M.A. Cusanovich, Biochim. Biophys. Acta 1187 (1994) 277–288.